Materials Research Proceedings **25** (2023) 413-420 https://doi.org/10.21741/9781644902417-51

Optimization of the sheet hydroforming process parameters to improve the quality of reshaped EoL components

Antonio Piccininni[1, a *], Angela Cusanno[1,b], Giuseppe Ingarao[2,c], Gianfranco Palumbo[1,d] and Livan Fratini[2,e]

[1]Dept. of Mechanics, Mathematics and Management, Politecnico di Bari, Via Orabona 4, 70125 Bari

[2] Department of Engineering, University of Palermo, Viale delle Scienze, Palermo, 90128, Italy

[a]antonio.piccininni@poliba.it, [b]angela.cusanno@poliba.it, [c]giuseppe.ingarao@unipa.it, [d]gianfranco.palumbo@poliba.it, [e]livan.fratini@unipa.it

Keywords: Aluminium, Hydroforming, Optimization

Abstract. The reshaping of End-of-Life (EoL) components by means of sheet metal forming process has been considered largely attractive, even from the social and economic point of view. At the same time, EoL parts can be often characterized by non-uniform thicknesses or alternation of work-hardened/undeformed zones as the results of the manufacturing process. Such heterogeneity can hinder a proper reshaping of the EoL part and residual marks on the re-formed blanks can be still present at the end of the reshaping step. In a previous analysis, the authors evaluated the effectiveness of reshaping a blank with a deep drawn feature by means of the Sheet Hydroforming (SHF) process: it was demonstrated that residual marks were still present if the deep drawn feature was located in a region not enough strained during the reshaping step. Starting from this condition and adopting a numerical approach, additional investigations were carried out changing the profile of the load applied by the blankholder and the maximum oil pressure. Numerical results were collected in terms of overall strain severity and residual height of the residual marks from the deep drawn feature at the end of the reshaping step. Data were then fitted by accurate Response Surfaces trained by means of interpolant Radial Basis Functions, subsequently used to carry out a virtual optimization managed by a multi-objective genetic algorithm. Optimization results suggested the optimal value of the output variables to reduce the marks from the deep drawn feature without the occurrence of rupture.

Introduction

Production of just five key materials (steel, cement, paper, aluminum, and plastic) accounts for over half of all the greenhouse gas (GHG) emissions released by industry worldwide each year [1]. Primary aluminum production process is the most energy and emissions intensive among the aforementioned materials [2]. Aluminum production industry is responsible for about 3% of the world's 9.4 Gt of direct industrial CO_2 emissions in 2021 [3]. Since 1971, the global demand for aluminum has increased by nearly six times; although during the Covid-19 pandemic the aluminum production fell flat, it has since started growing quickly once again and global demand is likely to continue growing in response to increasing global population and GDP 2021 [3]. The main approach for reducing the primary production and decoupling the resource depletion from the economic growth is the implementation of Circular Economy Strategies [4].

The basic idea is to turn material scraps and End-of-Life (EoL) products/components directly into reusable materials or, better yet, into new products/components. Although recycling is the most commonly applied strategy when metals are concerned, it allows only the material out of a EoL components to be recovered. Actually, to further reduce the environmental impact of Industry sector it is necessary moving towards more virtuous Circular Economy strategies able to recover both material and function from EoL components. Specifically for metals, Cooper and Allwood

proposed a framework for metal reuse, in which four main strategies – relocation, cascade, remanufacturing, and reform/reshaping – are identified [5]. Remanufacturing and Reshaping envisages manufacturing processes to be applied to reuse EoL components. In this respect manufacturing scientists have to find to processes or rethink conventional processes for processing/reprocessing EoL components. In this respect sheet metal based components might represent a significant share of EoL sector. It is worth remarking that sheet metal based components account for a quite large share of the global semi-finished production. In the case of aluminum alloys, sheets (including strips, foil production) account for about 45% of the yearly global demand [6]. Therefore, finding out reuse options for sheet metal based EoL components would enable significant environmental impact reduction.

Overall the Reshaping/Reforming approach has been overlooked by the scientific community so far. Forming processes applied specifically as reuse strategy for sheet metal based components are covered in very few scientific papers so far. Brosius et al. [7] described in a review paper how a demounted automotive engine-hood can be reshaped into a rectangular sheet metal component by sheet hydroforming process. Takano et al. [8] applied Single Point Incremental Forming (SPIF) on a flattened sheet. The Reshaping they propose includes the flattening of a previously bent sheet and a subsequent incremental forming step. Some of the authors of the present paper have recently proposed a novel approach to reshape sheet metal based EoL components [9,10]. Specifically, SPIF was directly applied on a deep-drawn square box to change its shape. However, the SPIF approach presented by the authors allows to add a feature on an EoL components rather than providing a brand new shape. To tackle this challenge, the authors have recently proposed a new Reshaping idea based on Sheet Hydroforming (SHF) process. In this study the authors replicated a reshaping route: a deep drawing process was adopted to impart a square feature; subsequently, SHF was performed to remove the feature and obtain a brand new shape. Results proved that hydroforming can be successfully applied for reshaping proposes [11]. Nevertheless, the developed analyses revealed that reshaping process design is more challenging than conventional forming one as new design objectives and constraints need to be considered making the process engineering more complex. The present paper, propose a multi objective design methodology addressed to the new design challenges characterizing Reshaping by hydroforming processes.

Methodology

A deep drawn aluminum blank (AA5754 H22, initial thickness equal to 0.5 mm) was considered as the EoL component to be completely reshaped by means of the hydroforming process, as shown in Fig. 1. The hydroforming already proved to be a suitable technological solution to give a new shape to the mentioned EoL component [11]. Nevertheless, it was also reported that when the deep drawn feature is located in the BOTTOM position – i.e. in the blank portion that comes in contact with the shallow step of the die cavity – its removal at the end of the reshaping step was much more complicated. As a consequence, using the same numerical scheme of previous analyses by the same authors, the main process parameters of the reshaping step – i.e., the maximum oil pressure and the blankholder force (BHF) – were optimized. In this way, the final geometry of the hydroformed part was improved and the residuals of the deep drawn feature removed as much as possible.

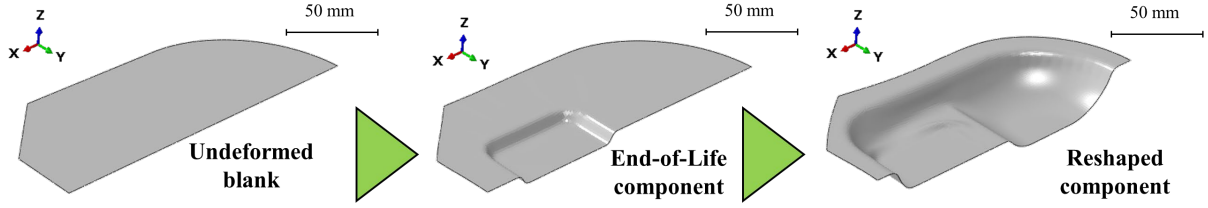

Fig. 1 The sequence of the simulated manufacturing steps

Materials Research Proceedings **25** (2023) 413-420 https://doi.org/10.21741/9781644902417-51

The numerical approach is briefly recalled in the following. The deep drawing step and the reshaping by hydroforming were simulated using the commercial code Abaqus (explicit solver) along with the springback analysis, modelling half of the system and using the mass scaling approach to speed up the numerical runs. The reliability of the numerical results was ensured by checking that the system's kinetic energy resulted always negligible (less than 20%) with respect to the system's internal energy. Tools were modelled as discrete three-dimensional (3D) shell rigid bodies, whereas the blank as a 3D shell deformable body (5 through-thickness integration points) and meshed using 4-node and 3-node triangular shell elements with reduced integration and hourglass control (S4R and S3R, respectively) with an average mesh size of 1 mm. Friction was modelled using the Coulomb's formulation and setting the coefficient to 0.125 [12] . Flow stress curve and Forming Limit Curve (FLC) [11] were implemented in the FE model; the latter allowed to activate a damage criterion - i.e., FLC damage initiation criterion (FLDCRT) - according to which when output variable FLDCRT overcame the threshold value of 1, the model predicted the occurrence of rupture.

a)

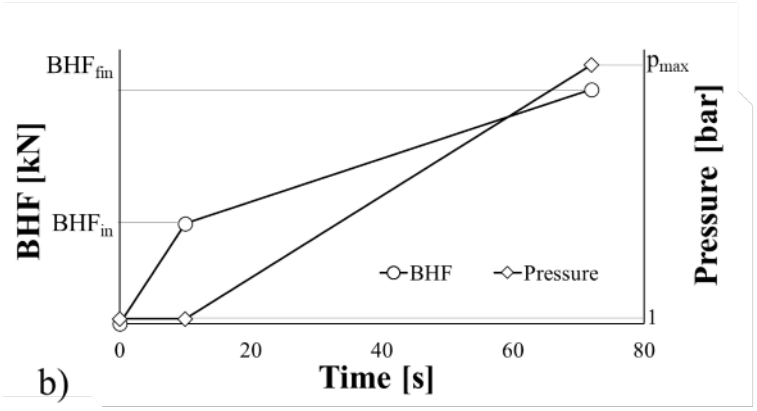

b)

ID	BHF$_{in}$	BHF$_{fin}$	BHF$_{avg}$	P$_{max}$
1	23	87	55	52
2	23	87	55	104
3	23	87	55	156
4	23	87	55	208
5	33	97	65	52
6	33	97	65	104
7	33	97	65	156
8	33	97	65	208
9	43	107	75	52
10	43	107	75	104
11	43	107	75	156
12	43	107	75	208
13	53	117	85	52
14	53	117	85	104
15	53	117	85	156
16	53	117	85	208

c)

Fig. 2 Additional FE runs: a) the reference ID06 working condition [11]; b) BHF and oil pressure profiles and c) list of the investigated reshaping conditions.

In the present work, 16 conditions were numerically investigated starting from the reference one, labelled as ID06 in [11] and shown in Fig. 2a, which was characterized by the deep drawn feature located in the bottom position, the BHF linearly increasing from 13 to 77 kN and the oil pressure up to 52 bar (with a pressure rate of 1 bar/s). The investigated conditions were arranged according to a full factorial plan changing only the process parameters related to the reshaping by hydroforming. In particular, the forming time was kept unchanged and the initial and final values of the BHF increased over 4 levels; on the other hand, the maximum oil pressure was increased up to 208 bar. Fig. 2b shows the simulated linear profiles of the mentioned process parameters, whereas Fig. 2c reports the list of the simulated conditions. Numerical results were analyzed in terms of the maximum value of the FLDCRT variable over the whole blank FLDCRT$_{max}$ and the height of the residual from the residual deep drawn feature (DelH), graphically explained in Fig. 3. The so-collected data were then used to train accurate Response Surfaces (RS) using the Radial

Basis Functions (RBF) interpolant algorithms available in the modeFRONTIER integration platform. More in details, the data set was initially subdivided into the training set (containing 90% of the 16 designs) and the validation set (based on the remaining 10%). RS were trained on the training set and their accuracy checked on the validation set; subsequently, they were used as the base for the virtual optimization aimed at simultaneously minimizing $FLDCRT_{max}$ and the DelH variables. The virtual optimization, managed by a multi-objective genetic algorithm (MOGA-II) evolved throughout 1000 successive generations.

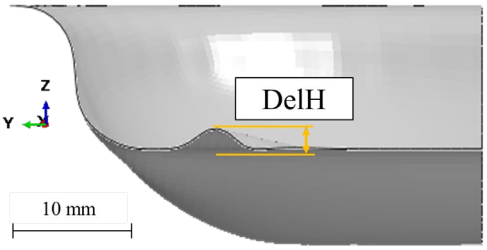

Fig. 3 Definition of the DelH output variable

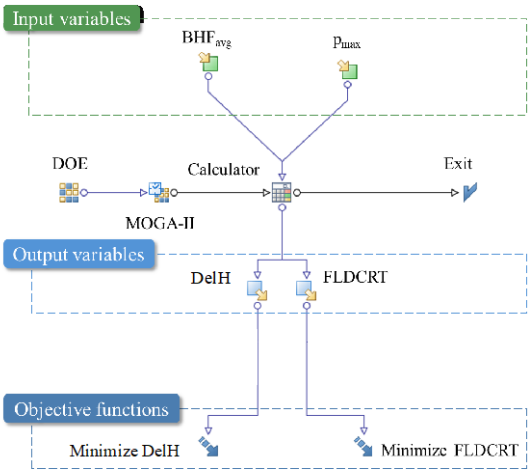

Fig. 4 Workflow of the optimization procedure

The workflow describing the virtual optimization procedure based on the trained RS is schematically shown in Fig. 4. At the end of the optimization round, optimal designs could be evaluated, represented by the average values of BHF and p_{max} which allowed to balance a significant reduction of the deep drawn feature without leading to a premature fracture of the component (i.e., a FLDCRT value lower than 1).

Results

Response Surfaces (RS) were created on the so-called "training set" containing approximately 90% of the DoE data set.. Among the five Radial Basis Functions available for the training of the RS, the Duchon's Polyharmonic Splines algorithm was chosen as the most precise on the DelH output variable, as shown by the errors and the R-squared values calculated on the "validation set" (containing the remaining 10% of the data set) and listed in Tab. 1.

Table 1 Evaluation of the RBF algorithms' fitting capabilities (DelH output variable): Duchon's Polyharmonic Spline (PS), Wendland's Compactly Supported (CS), Hardy's MultiQuadrics (MQ), Inverse MultiQuadrics (IMQ), Gaussians (G).

RBF Algorithm	Mean Absolute Error	Mean Relative Error	Mean Normalized Error	R-squared
PS	2.32E-2	1.90E-2	3.62E-2	0.993
CS	4.81E-2	3.18E-2	7.52E-2	0.973
MQ	5.41E-2	3.64E-2	8.46E-1	0.967
IMQ	8.92E-2	5.88E-2	1.39E-1	0.905
G	1.49E-1	1.01E-1	2.33E-1	0.756

As for the second output variable ($FLDCRT_{max}$), the Wendland's Compactly Supported resulted to be the most accurate RBF algorithm (as proved by the data listed in Tab. 2).

Table 2 Evaluation of the RBF algorithms' fitting capabilities (FLDCRT$_{max}$ output variable): Duchon's Polyharmonic Spline (PS), Wendland's Compactly Supported (CS), Hardy's MultiQuadrics (MQ), Inverse MultiQuadrics (IMQ), Gaussians (G).

RBF Algorithm	Mean Absolute Error	Mean Relative Error	Mean Normalized Error	R-squared
CS	1.51E-2	2.02E-2	4.54E-2	0.991
MQ	1.89E-2	2.18E-2	5.69E-2	0.977
IMQ	3.75E-2	4.52E-2	1.13E-1	0.922
PS	3.95E-2	6.75E-2	1.19E-1	0.909
G	7.31E-2	9.10E-2	2.20E-1	0.734

As Fig. 5a suggests, increasing the load applied by the blankholder and the maximum oil pressure leads to a more effective annihilation of the feature from the previous manufacturing step. Nevertheless, higher values of the input parameters may result detrimental for the outcome of the process since those operative conditions may lead to the blank rupture (FLDCRT higher than one) as confirmed by the RS in Fig. 5b.

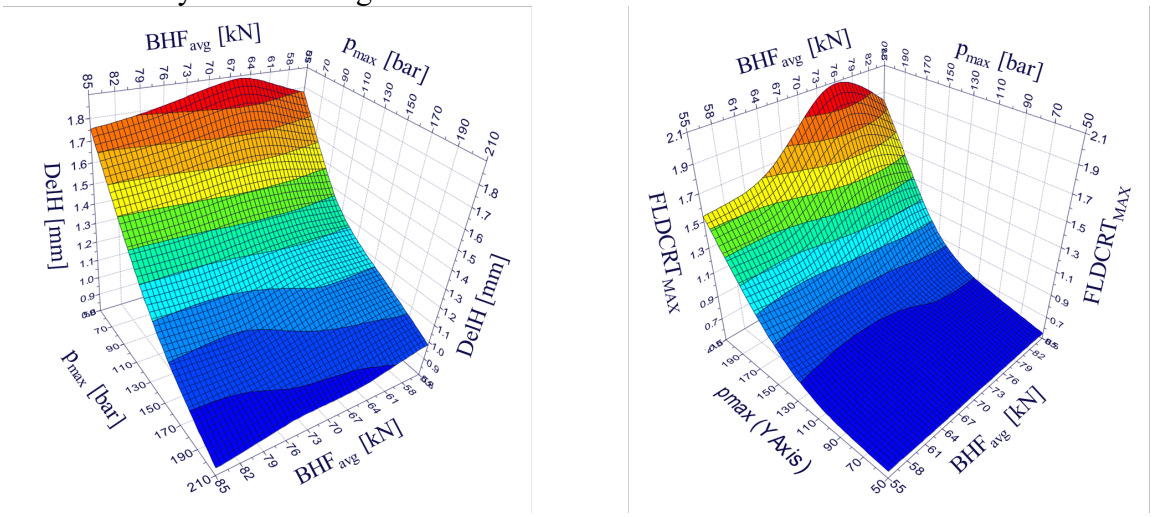

a) b)

Fig. 5 Trained response surfaces (RS) on the output variables: a) DelH and b) FLDCRTmax

The indications coming from the trained RS were absolutely in line with the general guidelines formulated by the authors in a previous work [11]: any evidence from the previous manufacturing step – if located in a blank region that is not going to be excessively deformed during the reshaping step – can be eliminated if the blank is more severely stretched during the second manufacturing step, which means to increase the load exerted by the blankholder or, alternatively, the maximum oil pressure. Nevertheless, such conditions may not be favorable for the overall soundness of the final component: in fact, an increase in the restraining forces may more easily lead to the occurrence of rupture over the blank region in contact with the deeper step of the die cavity. The RS were subsequently used as the base of a virtual optimization, managed by a multi-objective genetic algorithm (MOGA-II) [13]. On each of the defined output variable, a single objective function was defined with the final aim of minimizing simultaneously the FLDCRTmax and the DelH. In such a way, the optimization procedure would have led to the definition of the working window in which the residuals from the previous manufacturing step could be minimized without the occurrence of rupture in the reshaped blank.

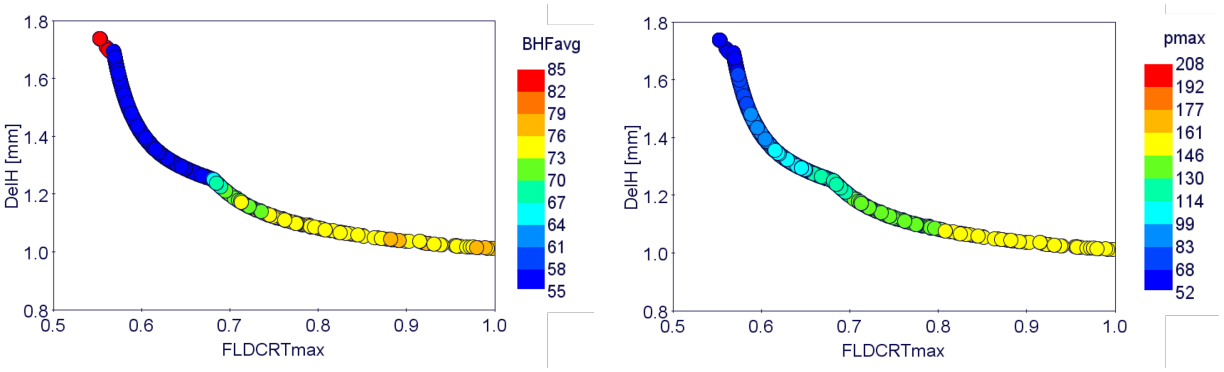

a) *b)*

Fig. 6 Pareto designs showing the optimal conditions in terms of a) BHFavg and b) pmax

The Pareto front is shown in Fig. 6 (a and b) collecting all the design considered optimal, i.e. capable of satisfying the two mentioned objective functions. The distribution of the Pareto designs is limited to conditions leading to maximum values of the FLDCRT variable lower than 1 (i.e., all those conditions leading to a final sound component). The result of the optimization suggests that if the final goal is to reduce as possible the appearance of the feature from the previous step without the occurrence of rupture, an average value of BHF_{avg} between 75 and 80 kN and a maximum pressure around 150 bar has to be set. The height of the feature is reduced down to 1 mm and the formed component is globally sound. To evaluate the accurateness of the optimization prediction, one of the Pareto designs (BHF_{avg} equal to 75 kN and maximum oil pressure equal to 160 bar) was simulated. The comparison between the numerical results (in terms of maximum FLDCRT and DelH) and the predicted values, shown in Fig. 7, clearly confirms the accuracy of the predicted optimized values (and, in turns, of the trained RS).

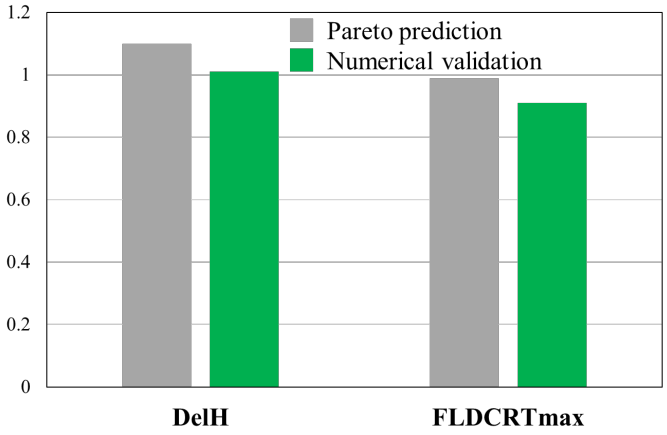

Fig. 7 Accuracy of the optimization prediction

Moreover, the optimized process parameters further confirmed their effectiveness when the appearance of the deep drawn feature at the end of the reshaping step was compared to the one from the ID06 (see Fig. 8, a and b): the increased oil pressure combined with higher restraining force led to the reduction of the DelH (from 1.8 mm to 1.1 mm) without affecting the soundness of the reshaped component (maximum FLDCRT lower than 1).

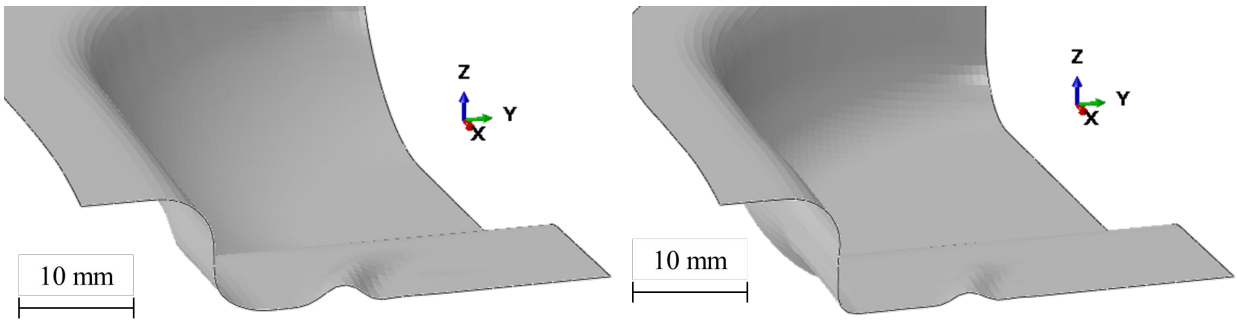

a) b)

Fig. 8 Appearance of the deep drawn feature at the end of the reshaping step: a) refernce ID06 condition and b) optimal Pareto condition

Conclusions

In the present paper, a follow-up of the reshaping methodology has been presented. In particular, starting from a condition characterized by the deep drawn feature located in the bottom positions, the hydroforming process parameters were varied to investigate the possibility of optimizing the blankholder force and the maximum oil pressure to completely remove the residuals from the deep drawn feature. Results from the optimization round, computationally attractive since based on the virtual generation of designs based on accurate Response Surfaces, confirmed the guidelines the authors already formulated in the previous analyses. More in details, the removal of the existing feature is much more effective if the blankholder force and the maximum oil pressure is increased, mainly related to the more severe blank stretching. At the same time, the increase of the restraining force becomes detrimental since inducing a more severe strain conditions in the rest of the blank (where the stretching is more pronounced since being in contact with the deep step of the die cavity). It was then concluded that the overall quality of the reshaped component can be undoubtfully improved and the residual marks from the deep drawn feature can be reduced but not eliminated until the feature is located in the bottom position. In fact, if an increase of the blankholder force may reduce more evidently the deep drawn feature but the integrity of the reshaped component cannot be ensured. Overall it is worth remarking that reshaping processes rise new challenges at the design stages. Along with conventional design objectives (homogenous thinning distribution with absence of fracture, absence of wrinkling and springback distortions minimization), the quality in terms of existing feature removal need to be added as output indicator. Also, the feature might be placed just in a narrow zone of the components to be reshaped. For actual industrial parts, restraining forces differentiation coupled with optimization techniques might be mandatory for a correct implementation of Reshaping processes. Along with the technological challenges to be addressed, the cost effectiveness of such an approach might represent a further issue to be faced. As a matter of fact, it might happen that the costs of the needed operations prior to reshaping (safe disassembly, inspection and decocting) might be too high with respect the value of the recovered sheet metal based EoL component. In this respect, a thorough comparative cost analysis with respect conventional recycling route would provide more clarity about the industrial applicability of the reshaping approach.

References

[1] G. Oberhausen, Y. Zhu, D.R. Cooper, Reducing the environmental impacts of aluminum extrusion, Resour. Conserv. Recycl. 179 (2022) 106120. https://doi.org/10.1016/j.resconrec.2021.106120

[2] M.F. Ashby, Materials and Environment, third ed., Butterworth-Heinemann, Oxford, 2021.

[3] Information on https://www.iea.org/reports/aluminium

[4] T. Tolio, A. Bernard, M. Colledani, S. Kara, G. Seliger, J. Duflou, Design, management and control of demanufacturing and remanufacturing systems, CIRP Ann. 66(2017) 585–609. https://doi.org/10.1016/j.cirp.2017.05.001

[5] D.R. Cooper, J.M. Allwood, Reusing Steel and Aluminum Components at End of Product Life, Environ. Sci. Technol., 46 (2012) 10334–40. https://doi.org/10.1021/es301093a

[6] J.M. Cullen, J.M. Allwood, Mapping the Global Flow of Aluminum: From Liquid Aluminum to End-Use Goods, Environ. Sci. Technol., 47 (2013) 3057–64. https://doi.org/10.1021/es304256s

[7] A. Brosius, M. Hermes, N.B. Khalifa, M. Trompeter, A.E. Tekkaya. Innovation by forming technology: motivation for research, Int. J. Mater. Form., 2 (2009) 29–38. https://doi.org/10.1007/s12289-009-0656-9

[8] H. Takano, K. Kitazawa, T. Goto, Incremental forming of nonuniform sheet metal: Possibility of cold recycling process of sheet metal waste, Int. J. Mach. Tools Manuf., 48 (2008) 477–82. https://doi.org/10.1016/j.ijmachtools.2007.10.009

[9] G. Ingarao, O. Zaheer, D. Campanella, L. Fratini, Re-forming end-of-life components through single point incremental forming, Manuf. Lett., 24 (2020) 132–5. https://doi.org/10.1016/j.mfglet.2020.05.001

[10] G. Ingarao, O. Zaheer, L. Fratini, Manufacturing processes as material and energy efficiency strategies enablers: The case of Single Point Incremental Forming to reshape end-of-life metal components, CIRP J. Manuf. Sci. Technol., 32 (2021) 145–53. https://doi.org/10.1016/j.cirpj.2020.12.003

[11] A. Piccininni, A. Cusanno, G. Palumbo, O. Zaheer, G. Ingarao, L. Fratini, Reshaping End-of-Life components by sheet hydroforming: An experimental and numerical analysis, J. Mater. Process. Technol. 306 (2022) 117650. https://doi.org/10.1016/j.jmatprotec.2022.117650

[12] J. Domitner, Z. Silvayeh, A. Shafiee Sabet, K.I. Öksüz, L. Pelcastre, J. Hardell, Characterization of wear and friction between tool steel and aluminum alloys in sheet forming at room temperature, J. Manuf. Process 64 (2021) 774–84. https://doi.org/10.1016/j.jmapro.2021.02.007

[13] S. Poles, E. Rigoni, T. Robič, MOGA-II Performance on Noisy Optimization Problems. Proc. Int. Conf. Bioinspired. Optim. Methods Their Appl. (2004) 51–62.